

# NASA Technical Memorandum

NASA TM-86509

## SPACE SHUTTLE MOLECULAR SCATTERING AND WAKE VACUUM MEASUREMENTS

By R. J. Naumann, G. R. Carignan and  
E. R. Miller

Space Science Laboratory  
Science and Engineering Directorate



June 1985

# NASA

National Aeronautics and  
Space Administration

George C. Marshall Space Flight Center

TECHNICAL REPORT STANDARD TITLE PAGE

1. REPORT NO. NASA TM- 86509		2. GOVERNMENT ACCESSION NO.		3. RECIPIENT'S CATALOG NO.	
4. TITLE AND SUBTITLE Space Shuttle Molecular Scattering and Wake Vacuum Measurements				5. REPORT DATE June 1985	
				6. PERFORMING ORGANIZATION CODE ES71	
7. AUTHOR(S) R. J. Naumann, G. R. Carignan,* and E. R. Miller				8. PERFORMING ORGANIZATION REPORT #	
9. PERFORMING ORGANIZATION NAME AND ADDRESS George C. Marshall Space Flight Center Marshall Space Flight Center, Alabama 35812				10. WORK UNIT NO.	
				11. CONTRACT OR GRANT NO.	
				13. TYPE OF REPORT & PERIOD COVERED Technical Memorandum	
12. SPONSORING AGENCY NAME AND ADDRESS National Aeronautics and Space Administration Washington, D.C. 20546				14. SPONSORING AGENCY CODE	
15. SUPPLEMENTARY NOTES Prepared by Space Science Laboratory, Science and Engineering Directorate. *Space Physics Research Laboratory, University of Michigan, Ann Arbor, Michigan.					
16. ABSTRACT <p>The wake environment of the space shuttle is analyzed to determine whether it is feasible to perform ultra-high vacuum experiments in or near the payload bay with the shuttle oriented such that the payload bay faces the anti-velocity direction. Several mechanisms were considered by which molecules could approach the payload bay from this direction and their relative contributions to the wake environment are estimated. These mechanisms include ambient atmospheric molecules that have velocities in excess of the orbital velocity which can overtake the shuttle, ambient atmospheric molecules that are backscattered by collisions with the shuttle-induced atmosphere, and self-scattering from the induced atmosphere.</p> <p>These estimates are compared with the measurements made with the collimated mass spectrometer which was part of the Induced Environment Contamination Monitor flown on several of the early shuttle flights. Although the collimated mass spectrometer was not designed for this purpose and the instrument background for the species for which the collimator is effective is above the expected levels, upper limits can be established for these species in the wake environment which are consistent with the analysis. There was considerably more helium and argon observed in the wake direction than was predicted, however. Possible origins of these gases are discussed.</p>					
17. KEY WORDS Ultrahigh Vacuum Molecular Wake Shield Molecular Scattering Spacecraft Contamination			18. DISTRIBUTION STATEMENT Unlimited--Unclassified <i>Robert Naumann</i>		
19. SECURITY CLASSIF. (of this report) Unclassified		20. SECURITY CLASSIF. (of this page) Unclassified		21. NO. OF PAGES 32	
				22. PRICE NTIS	

## TABLE OF CONTENTS

	Page
INTRODUCTION .....	1
SHUTTLE-INDUCED ENVIRONMENT MEASUREMENTS .....	2
BACKSCATTERING OF ATMOSPHERIC MOLECULES .....	4
BACKSCATTERING FROM COLLISIONS WITHIN THE INDUCED ATMOSPHERE .....	5
DISCUSSION OF RESULTS .....	10
CONCLUSIONS .....	11
APPENDIX A .....	13
APPENDIX B .....	17
REFERENCES .....	19

PRECEDING PAGE BLANK NOT FILMED

# LIST OF TABLES

Table	Title	Page
1.	Ambient Environment of an Orbiting Vehicle at 250 km .....	21
2.	Summary of Measured Environment of Various Missions .....	22
3.	Wake Environment Observed on STS-3 .....	23
4.	Measurements in STS-3 Payload Bay with Doors Closed .....	24
5.	Relative Scattering Efficiencies for Collisions of Interest .....	25
6.	Wake Environment from Ambient Molecules Backscattered by Collisions with Thermal Molecules in the Induced Environment .....	26
7.	Backscatter Function $F(\zeta_0, M)$ for $\zeta_0 = 0$ and $\zeta_0 = 0.2$ .....	27
8.	Comparison of Estimated and Measured Wake Environment .....	28

## TECHNICAL MEMORANDUM

### SPACE SHUTTLE MOLECULAR SCATTERING AND WAKE VACUUM MEASUREMENTS

#### INTRODUCTION

The use of space for the processing of materials is receiving renewed interest now that the space shuttle fleet can provide access to low-Earth orbit on a more or less routine basis. The experiments being carried out at present utilize the microgravity aspect of orbital flight which provides a unique environment that can only be obtained for extended periods in spaceflight.

Another aspect of spaceflight that may also be useful for the processing of materials is the use of space vacuum [1-3]. The residual atmosphere at shuttle altitudes (250-300 km) is on the order of  $10^9$  molecules/cm<sup>3</sup> which corresponds to pressures on the order of  $10^{-7}$  Torr ( $10^{-5}$  Pascals) which is only a modest vacuum. However, orbital velocity is several times greater than the mean thermal speeds of the residual atmospheric molecules. Therefore the pressure observed from an orbiting spacecraft will have a strong anisotropy, as may be seen in Table 1. The values in Table 1 are calculated from the maximum densities [4] of atmospheric constituents at 250 km with a temperature of 1000 K and therefore represent worst-case estimates. The estimated wake fluxes are obtained by integrating the directional flux from a drifting Maxwell-Boltzmann gas over the wake hemisphere (see Appendix A). These calculations assume no scattering or other interactions between the atmospheric molecules and molecules leaving the spacecraft. Such interactions can significantly alter these fluxes as will be shown in this paper.

If the off-gassing or other molecular sources from the spacecraft can be kept sufficiently low so that the vacuum levels indicated in Table 1 can be approached, it would appear that the wake vacuum would be useful for a variety of applications where extremely high vacuums must be maintained. The most prevalent residual gases are He and atomic H from the high-speed tail of the Maxwell-Boltzmann distribution that can overtake the spacecraft. Heavier molecules such as O<sub>2</sub>, N<sub>2</sub>, H<sub>2</sub>O, etc. are virtually non-existent. Since such a system exhausts into half the universe, the pumping speed is virtually infinite and there are no walls to reflect unwanted contaminants. Heat can be rejected by radiating into space which acts as a 4 K sink. None of these capabilities are truly unique; they can be duplicated on Earth if sufficient care is taken. But it may eventually turn out to be simpler and more economical to carry out processes that require better than  $10^{-12}$  Torr vacuum in conjunction with high heat and/or gas loads in the wake of a suitable orbiting vehicle.

Such a facility was proposed several years ago by Melfi and Outlaw at NASA Langley [5]. After several years of feasibility study, NASA elected to postpone any additional development of the concept until the user community showed a more definite interest. The Langley concept involved a large (3-5 m) shield that would be tethered or mounted on a boom several tens of meters away from the shuttle. This would reduce the scattering of molecules into the wake vacuum region from the shuttle-induced environment.

A much simpler alternative for more modest vacuum requirements would be to use the shuttle itself as the wake shield. By flying with the belly in the ram direction, the payload bay becomes a wakeshield vacuum facility of sorts. Of course the shuttle represents a large source of molecular contaminants, but most of these molecules will be moving away from the payload bay with little chance of returning. Therefore, it would seem that an experiment suitably protected from these outgoing molecules could attain a reasonably high vacuum level. The vacuum level that can be attained depends primarily on the shuttle-induced environment and its interactions with the ambient environment. Since such things are difficult to predict, reliable estimates of the vacuum levels that could be reached in the payload bay cannot be made apriori. However, since the shuttle-induced environment was of concern to the shuttle users community, NASA undertook a measurement program on the first several shuttle flights to characterize this environment.

The purpose of this paper is to summarize what has been learned about the shuttle-induced environment and to attempt to place rough order-of-magnitude estimates on the vacuum levels in the payload bay for the purpose of assessing the feasibility of using the shuttle as a wake vacuum facility.

#### SHUTTLE-INDUCED ENVIRONMENT MEASUREMENTS

The first several shuttle flights carried an instrument package referred to as the Induced Environment Contamination Monitor (IECM) to assess the particle and gases environment in and around the payload bay [6]. Included in this instrument package was a quadrupole mass spectrometer similar to the spectrometers flown on Dynamics Explorer and Atmospheric Explorer [7]. One of the primary concerns about the shuttle environment was the induced  $H_2O$  column density from outgassing, water dumps, flash evaporator operation, and thruster firings. To obtain information on the column density of  $H_2O$  and other species that absorb radiation in wavelengths of interests to astronomers, a collimator was placed in front of the mass spectrometer to restrict its acceptance to a cone of  $10^\circ$  half-angle or 0.1 steradian solid angle. The backscattered flux was measured at small angles relative to the velocity vector and the column density was computed from elementary scattering theory.

The collimator is shown in Figure 1. It consists of three skimmers with getters to trap the off-axis molecules. This technique worked quite well for the measurements of primary interest. However, the subsequent off-gassing of the molecules trapped by the getters provides an instrument background that is higher than the expected wake environment for some species; hence, the fluxes and equivalent partial pressures of the trapped species in the wake region cannot be obtained directly. Some direct measurement of noble gases such as He and Ar are possible since they are not gettered by the zirconia. Other mass spectrometers have also been flown on early shuttle missions, but they were not oriented relative to the payload bay to observe the wake flux [8-9].

The observed ram-to-wake ratios for He are given in Table 2 along with the wake measurements. The ram measurements correspond to atmospheric concentration of He [10]. Also shown in Table 2 is the  $H_2O$  column density inferred from the mass spectrometer backscatter measurements. Note the large variations from mission to mission. (There are also variations during a particular mission; the values presented here are representative after an initial off-gassing period.) STS-2 was

subjected to heavy rain prior to launch, and the porous tiles used in the thermal protection system may have carried large amounts of  $H_2O$  into orbit. STS-3 had a thicker water-resistant coating and was by far the "cleanest" flight monitored in terms of gaseous background. Also it was flown in an inertial attitude for most of the mission such that the shuttle z-axis (normal to the payload bay) usually came within 10-20 degrees of both the wake and ram direction during an orbital revolution. This accounts for the stronger ram/wake modulation than was seen on other missions. STS-4 carried instruments that evolved  $N_2$  and He which probably accounted for the high level of He. It was also subjected to heavy rain and some hail damage prior to flight. In addition, the survey conducted by the IECM attached to the remote manipulator arm detected a significant leak in the freon cooling system which could effectively backscatter atmospheric molecules into the wake. Spacelab 1 contained the large manned Spacelab module with its various fluid loops, multilayer insulation, paint, etc. that was exposed to space vacuum for the first time. Also, on this flight the IECM along with a number of other instruments was located on a pallet between the aft bulkhead and the Spacelab module which was partially in the field-of-view of the mass spectrometer. Therefore, molecules reflected from these surfaces contribute to the measurement. The Dynamics Explorer data are included to illustrate that extremely low vacuum levels can be achieved on the wake side of orbiting spacecraft.

The STS-3 mission appears to represent what is possible to achieve on the shuttle as a wake vacuum facility if only modest care is taken to reduce the induced environment. Table 3 shows the partial pressures of various species observed in the wake configuration during this mission. Except for He and A these measurements are instrument background and, therefore, represent upper limits on the wake environment. We will attempt to estimate the wake environment for species other than He by indirect observations. Near the end of the mission the payload bay doors were closed and the mass spectrometer observed a rise in partial pressure of a number of species to equilibrium pressures shown in Table 4. This equilibrium is a result of molecules leaving the payload bay through the side vents (total area =  $0.76 \text{ m}^2$ ) at the same rate they are evolving from various sources in the payload bay. From this consideration the source functions in Table 4 are estimated by assuming that molecules evolve uniformly from the payload bay area ( $86 \text{ m}^2$ ) at the rate they are pumped by the side vents.

The column densities for each of these species with the payload bay doors open is estimated by assuming the source is distributed over a flat disc with area equivalent to the payload bay, which acts as a Lambertian emitter (see Appendix B). Integrating the contribution from each element of the disc along the vertical axis from an observation point  $z_0$  above the plane of the disc to infinity (ignoring particles lost by scattering) the column density is given by

$$N_c = \frac{8Q}{\pi \langle v \rangle} \left[ (z_0^2 + R_0^2)^{1/2} - z_0 \right] \quad (1)$$

where  $Q$  is the distributed source strength,  $\langle v \rangle$  is the average molecular speed, and  $R_0$  is the radius of the disc. The IECM mass spectrometer is located approximately 1 m above the sill line of the payload bay which has an equivalent radius of 5.23 m.

Note that the column density for  $H_2O$  obtained by this estimate is roughly an order of magnitude lower than the value inferred from the backscatter measurements in Table 2. This is because only sources of  $H_2O$  in the payload bay are considered

in this estimate. External sources such as outgassing from the tiles, thruster firings, flash evaporator operation, etc. would not be included in this estimate.

#### BACKSCATTERING OF ATMOSPHERIC MOLECULES

Using the column density estimates in Table 4, the contribution from atmospheric backscatter to the wake environment may be estimated. From elementary scattering theory it can be shown that the scattered flux incident on a surface arriving from an element of solid angle  $d\Omega$  oriented at angle  $\theta$  with respect to the velocity vector and  $\phi$  relative to the surface normal is,

$$\frac{\partial \Phi_i(\theta, \phi)}{\partial \Omega} = n_A v_A N_C(\phi) \cos \phi \left( \frac{\partial \sigma_i}{\partial \omega} \right)_{\theta}, \quad i = A, O \quad (2)$$

where  $n_A v_A$  is the ambient flux,  $N_C$  is the induced column density,  $(\partial \sigma_i / \partial \omega)_{\theta}$  is the differential scattering cross section, and the subscript  $i$  refers to ambient or outgassing molecules. The differential scattering cross section may be approximated by assuming the outgassing molecules are at rest and are being struck by ambient molecules moving at orbital velocity. The expression is

$$\left( \frac{\partial \sigma}{\partial \omega} \right)_{\theta} = \frac{\sigma_{AO}}{4\pi} \left[ \frac{1 + \beta_i^2 (\cos^2 \theta - \sin^2 \theta)}{(1 - \beta_i^2 \sin^2 \theta)^{1/2}} + 2\beta_i \cos \theta \right] \quad (3)$$

where  $\beta_A = m_A m_O^{-1} \epsilon^{-1/2}$ ,  $\beta_O = \epsilon^{-1/2}$ ,  $m_A$  and  $m_O$  are the masses of the colliding molecules,  $\sigma_{AO}$  is the total molecular collision cross section, and  $\epsilon$  is the coefficient of restitution (kinetic energy after the collision/kinetic energy before the collision).

Note that for  $\beta_i = 1$  this expression reduces to

$$\left( \frac{\partial \sigma}{\partial \omega} \right)_{\theta} = \frac{\sigma_{AO}}{4\pi} \begin{cases} 4 \cos \theta, & 0 \leq \theta \leq \pi/2 \\ 0, & \pi/2 < \theta \leq \pi \end{cases} \quad (4)$$

For  $\beta > 1$  real values for  $(\partial \sigma / \partial \omega)$  exist only for  $\theta < \pi/2$ . Hence no outgassing molecule can be scattered at angles greater than  $90^\circ$ , which means molecules leaving the payload bay in the wake configuration cannot return as a result of single collisions with the ambient molecules.\* On the other hand, ambient molecules can be scattered into the wake region by collisions with outgassing molecules provided  $m_A/m_O < \epsilon^{1/2}$ .

\*Since mean-free-paths at shuttle altitudes are on the order of 100 meters, multiple collisions need not be considered.



To estimate the amount of this scattering,  $\theta$  is set equal to  $\pi - \phi$ , which corresponds to the surface in question being oriented in the anti-velocity direction, and equation (2) is integrated over the wake hemisphere. The column density estimate from the closed payload bay measurements is along the vehicle axis. If the source is assumed to be Lambertian, the column will have a cosine dependence, hence  $N_C(\phi) = N_C \cos \phi$ . The total flux of ambient molecules of species A scattered into the wake region by outgassing species  $\theta$  is given by

$$\Phi_{A,O} = 2\pi n_A v_A N_C \int_0^{\pi/2} \cos^2 \phi \sin \phi \left( \frac{\partial \sigma_A}{\partial \omega} \right)_{\pi-\phi} d\phi. \quad (5)$$

The integral involves elliptic functions and was evaluated numerically. The results for the various interactions of interest are tabulated in Table 5 assuming elastic collisions ( $\epsilon = 1$ ). These results are normalized by dividing each  $\Phi_{A,O}$  by  $\Phi_{A,\infty}$  and may be thought of as a relative scattering efficiency for the collision in question as compared to a collision in which  $m_A \ll m_O$ . As  $m_A/m_O \rightarrow 0$ ,  $(\partial \sigma_1 / \partial \omega)_\theta \rightarrow \sigma_{AO}/4\pi$ , and the flux  $\Phi_{A,\infty}$  is given by

$$\Phi_{A,\infty} = \frac{1}{6} n_A v_A N_C \sigma_{A,O}. \quad (6)$$

Using an average molecular diameter of  $3 \times 10^{-8}$  cm,  $\sigma_{A,O} = 2.8 \times 10^{-15}$  cm<sup>2</sup>. Using the number densities at 250 km in Table 1 and the estimated column densities in Table 4,\* the backscattered atmospheric flux is computed by multiplying equation (6) by the normalized scattering efficiencies in Table 5 and summing over each possible collision pair. The results are shown in Table 6.

For small acceptance angles typical of the collimated mass spectrometer, equation (5) reduces to

$$\Delta \Phi_{A,O} = n_A v_A N_C \frac{\sigma_{A,O}}{4\pi} (1 - \beta_1^2) \Delta \Omega, \quad (7)$$

where  $\Delta \Omega$  is the solid angle of instrument acceptance. This expression was used to compute the directional flux at  $\theta = \pi$  in Table 6.

#### BACKSCATTERING FROM COLLISIONS WITHIN THE INDUCED ATMOSPHERE

Consider an element of volume  $dV$  located some distance  $z$  above the observation point. The number of collisions per unit time between species 1 and 2 that scatter molecules of species 1 into solid angle  $d\omega$  is given by

$$d\dot{N}_1 = n_1 n_2 \langle v_{12} \rangle dV \left( \frac{\partial \sigma_{12}}{\partial \omega} \right)_\alpha d\omega \quad (8)$$

\*Except for H<sub>2</sub>O whose column density was taken from Table 2.

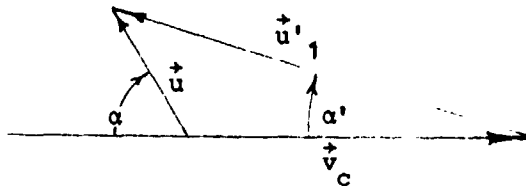
where  $n_1$  and  $n_2$  are the number densities of the two species,  $\langle v_{12} \rangle$  is the average relative velocity, and  $(\partial \sigma_{12} / \partial \phi)_\alpha$  is the directional scattering cross section for direction  $\alpha$ .

If both molecules are moving away from the spacecraft, the center of mass has a net positive velocity in that direction, and the average velocity is given by

$$\vec{v}_c = \frac{m_1 \vec{v}_1 + m_2 \vec{v}_2}{m_1 + m_2} \quad (9)$$

where  $m_1$  and  $m_2$  are the respective masses and  $\vec{v}_1$  and  $\vec{v}_2$  are the average velocities of the two components.

Elastic collisions in the center-of-mass system scatter isotropically and the magnitudes of the original velocities are retained; i.e.,  $|\vec{u}'_1| = |\vec{v}'_1|$  and  $|\vec{u}'_2| = |\vec{v}'_2|$  where  $\vec{u}'_1$  and  $\vec{u}'_2$  are the post-collision velocities and the primes denote center of mass reference. The scatter angle  $\alpha$  in the lab system is related to  $\alpha'$  in the center-of-mass system by the vector diagram.



From the law of sines,

$$\frac{\sin(\alpha - \alpha')}{v_c} = \frac{\sin(\pi - \alpha)}{u'_1} \quad (10)$$

or

$$\tan \alpha = \frac{u'_1 \sin \alpha'}{u'_1 \cos \alpha' - v_c} \quad (11)$$

For small  $\alpha$

$$\alpha = \frac{u'_1 \alpha'}{u'_1 - v_c} \quad (12)$$

Since

$$\begin{aligned} \left( \frac{\partial \sigma}{\partial \omega} \right)_{\alpha} d\omega &= \left( \frac{\partial \sigma}{\partial \omega} \right)_{\alpha'} d\omega', \quad \left( \frac{\partial \sigma}{\partial \omega} \right)_{\alpha'} = \frac{\sigma_{12}}{4\pi}, \text{ and } |u'_1| = |v'_1|, \\ \left( \frac{\partial \sigma}{\partial \omega} \right)_{\alpha \ll 1} &= \frac{\sigma_{12}}{4\pi} \frac{\sin \alpha' d\alpha'}{\sin \alpha d\alpha} = \left\{ \frac{\sigma_{12}}{4\pi} \left[ \frac{v'_1 - v_c}{v'_1} \right]^2, \quad v'_1 > v_c, \right. \\ &\quad \left. 0, \quad \text{otherwise} \right\} \end{aligned} \quad (13)$$

Note that  $v'_1 > v_c$  in order to backscatter into angle  $\alpha$ . Let the detector area  $dA$  subtend  $d\omega$  at  $z$ , hence  $d\omega = dA/z^2$ . Also note that  $dV$  can be written  $z^2 d\Omega dz$ . Making these substitutions into equation (8) along with the result of equation (13),

$$d\dot{N}_1 = n_1 n_2 \langle v_{12} \rangle z^2 d\Omega dz \frac{\sigma_{12}}{4\pi} \left[ \frac{v'_1 - v_c}{v'_1} \right]^2 \frac{dA}{z^2}. \quad (14)$$

Since  $\dot{\Phi}_1 = d\dot{N}_1/dA$ , the contribution from  $dz$  to the directional flux scattered opposite to the center-of-mass velocity may be written,

$$\frac{d}{dz} \left( \frac{\partial \Phi}{\partial \Omega} \right)_{c/m} = n_1 n_2 \langle v_{12} \rangle \frac{\sigma_{12}}{4\pi} \left( 1 - v_c/v'_1 \right)^2. \quad (15)$$

For simplicity's sake and since the center-of-mass velocity is predominantly in the  $z$ -direction, we will approximate  $(\partial \Phi / \partial \Omega)_{c/m} \approx (\partial \Phi / \partial \Omega)_z$ . Now it remains to express  $v'_1$ ,  $v_c$ ,  $n_1$ , and  $n_2$  in terms of  $r$  and  $z$  and integrate to obtain the directional backscatter. The velocity of the center of mass can be expressed as

$$\vec{v}_c = \left[ \frac{m_1 v_{1x} + m_2 v_{2x}}{m_1 + m_2} \right] \hat{i} + \left[ \frac{m_2 v_{2y}}{m_1 + m_2} \right] \hat{j} + \left[ \frac{m_1 v_{1z} + m_2 v_{2z}}{m_1 + m_2} \right] \hat{k} \quad (16)$$

where  $\hat{i}$ ,  $\hat{j}$ ,  $\hat{k}$  and are unit vectors and the  $x$ -axis is chosen as the direction of the radial component of the velocity of particle 1. The  $\vec{v}'_1$  is given by

$$\vec{v}'_1 = \vec{v}_1 - \vec{v}_c = \frac{m_2}{m_1 + m_2} \left[ (v_{1x} - v_{2x}) \hat{i} + v_{2y} \hat{j} + (v_{1z} - v_{2z}) \hat{k} \right]. \quad (17)$$

The ratio of  $v_c/v'_1$  can be written

$$\frac{v_c}{v'_1} = \left[ \frac{M^2 v_1^2 + v_2^2 + 2M v_{1z} v_{2z} + 2M v_{1x} v_{2x}}{v_1^2 + v_2^2 - 2 v_{1z} v_{2z} - 2 v_{1x} v_{2x}} \right]^{1/2} \quad (18)$$

where  $M = m_1/m_2$ .

This expression should be inserted into equation (15) which, in turn, should be integrated over all possible source locations and then averaged over the velocity distributions of  $v_1$  and  $v_2$ . However, to obtain order-of-magnitude estimates, we will insert average values for  $v_1^2$  and  $v_2^2$ , ignoring the small errors resulting from the fact that  $\langle v^2 \rangle \neq \langle v \rangle^2$ . To avoid having to integrate over all possible sources of both particles, average values for  $v_{2x}$  and  $v_{2z}$  are also used.

The  $\langle v_{2z} \rangle$  is obtained by

$$\langle v_{2z} \rangle = \int_0^{R_0} \langle v_2 \rangle \frac{z}{(r^2 + z^2)^{1/2}} dn_2 / \int_0^{R_0} dn_2, \quad r^2 = x^2 + y^2. \quad (19)$$

It is shown in Appendix A that

$$dn = 2Q \langle v^{-1} \rangle \frac{r z}{(r^2 + z^2)^{3/2}} dr.$$

Using this,

$$\langle v_{2z} \rangle = \frac{\langle v_2 \rangle}{2} \frac{R_0^2}{R_0^2 + z^2 - z(R_0^2 + z^2)^{1/2}}. \quad (20)$$

Note that for  $z \ll R_0$ ,  $\langle v_{2z} \rangle \rightarrow \langle v_2 \rangle / 2$  and for  $z \gg R_0$ ,  $\langle v_{2z} \rangle \rightarrow \langle v_2 \rangle$ .

The radial component of  $\vec{v}_2$  is given by  $v_{2r} = [v_2^2 - v_{2z}^2]^{1/2}$ . The  $v_{2x}$  component is given by  $v_{2r} \cos \lambda$  where  $\lambda$  is the azimuthal direction. The majority of the contribution comes from opposing collisions, i.e.,  $v_{2x} < 0$  (indeed for  $M > 1$  this must be case for  $v_c < v_1'$ ); therefore, the average is taken as

$$\langle v_{2x} \rangle = - \int_{-\pi/2}^{\pi/2} v_{2r} \cos \lambda \frac{d\lambda}{\pi} = - \frac{2}{\pi} [\langle v_2^2 \rangle - \langle v_{2z}^2 \rangle]^{1/2}. \quad (21)$$

The number density of species 2 at height  $z$  may be estimated from

$$n_2(z) = \int_0^{R_0} dn_2 = \frac{N_{c2}}{R^*} \int_0^{R_0} \frac{zr dr}{(z^2 + r^2)^{3/2}} = \frac{N_{c2}}{R^*} \left[ 1 - \frac{z}{(R_0^2 + z^2)^{1/2}} \right] \quad (22)$$

where  $R^* = (R_o^2 + z_o^2)^{1/2} - z_o$ . Using the same expression for  $dn_1$  equation (15) becomes

$$\frac{\partial \phi_1}{\partial \Omega} = \frac{\sigma_{12} N_{c1} N_{c2} \langle v_{12} \rangle}{4\pi R_o [(1 + \zeta_o^2)^{1/2} - \zeta_o]^2} \int_{\zeta_o}^{\infty} \left[ 1 - \frac{\zeta}{(1 + \zeta^2)^{1/2}} \right] d\zeta$$

$$\int_0^1 \left( 1 - \frac{v_c}{v_1} \right)^2 \frac{\zeta \rho}{(\zeta^2 + \delta^2)^{3/2}} d\rho$$
(23)

where  $v_c/v_1$  is given by equation (18),  $\zeta = z/R_o$ ,  $\zeta_o = z_o/R_o$ , and  $\rho = r/R_o$ . This allows the directional backscatter to be written in the form

$$\frac{\partial \phi_1}{\partial \Omega} = \frac{\sigma_{12} N_{c1} N_{c2} \langle v_{12} \rangle}{4\pi R_o [(1 + \zeta_o^2)^{1/2} - \zeta_o]^2} F(\zeta_o, M)$$
(24)

where  $F(\zeta_o, M)$  is a dimensionless scattering function given by the integral in equation (23) that depends on the geometry and relative masses of the molecules.

Introducing the following relations,

$$v_2 = v_1 M^{1/2}$$

$$v_{1x} = v_1 r / (r^2 + z^2)^{1/2}$$

$$v_{1z} = v_1 z / (r^2 + z^2)^{1/2}$$

$$\text{and } \langle v_{12} \rangle = \left[ \frac{8kT(m_1 + m_2)}{\pi m_1 m_2} \right]^{1/2},$$

the integrations were carried out using Simpson's rule. For  $M \geq 1$ , contributions cease for  $z = R_o/2$ . Above this height the angles available to the colliding molecules are such that the heavier molecule can no longer be scattered backward. For  $M < 1$ , backscatter can occur at larger values of  $z$ . For  $z \gg R_o$ ,

$$v_c = (m_1 v_1 + m_2 v_2) / (m_1 + m_2),$$

$$v = m_2 (v_1 - v_2) / (m_1 + m_2)$$

and

$$\left(1 - \frac{v_c}{v_1}\right) + \frac{(1-M)v_1 - 2v_2}{v_1 - v_2}.$$

For thermal velocities,  $v_2 = v_1 M^{1/2}$  and

$$\left(1 - \frac{v_c}{v_1}\right) + \frac{1 - 2M^{1/2} - M}{1 - M^{1/2}}.$$

This term will remain positive provided  $M < 3 \cdot 2^{3/2}$  or  $m_2 > 5.82 m_1$ . In this case backscatter will be possible for all values of  $z$ . The integral becomes

$$F(\zeta_0, M) \rightarrow \frac{(1 - 2M^{1/2} - M)^2}{12 \zeta_0^3 (1 - M^{1/2})^2}$$

provided  $M < 3 \cdot 2^{3/2}$  and  $\zeta_0 \gg 1$ .

The values for the integral in equation (23) are given in Table 7 for various combinations of molecular collisions assuming  $z_0 = 0$  and  $z_0 = 0.2 R_0$  (shown in parentheses). Using the column density estimates in Table 4 (except for  $H_2O$ ) the backscattered directional flux is computed for each collision combination and summed to obtain the total directional backscatter flux for each species. The total return flux is estimated by multiplying the directional flux by  $\pi$ . The results are listed in Table 8 along with the wake environment from the ambient atmosphere and atmospheric backscattering from collisions with the induced atmosphere.

#### DISCUSSION OF RESULTS

The estimates of the various contribution to the wake environment are presented in Table 8 along with the measurements described previously. Note that the net partial pressures for  $H_2O$ ,  $N_2$ , and  $O_2$  are well below the upper limit values set by the instrument background due to the collimator. The most abundant species in the wake environment should be O which cannot be observed directly with the type of mass spectrometer used on the IECM because O atoms do not survive the multiple collisions in the ionization chamber. Instead O atoms form other molecules such as  $O_2$ , CO, and  $CO_2$  from such collisions. The measured upper limit for mass 28 is sufficient to account for both the expected  $N_2$  and the CO formed from such reactions.

The major discrepancies are in the comparison of the measured values of He and A with their expected values. Note that the measured value of He is more than an order of magnitude higher than estimated and A is more than 4 orders higher. It is difficult to understand how molecules as heavy as A could be backscattered by any of the mechanisms considered here.

The most likely source for these atoms would appear to be the aft bulkhead which subtends a small solid angle in the hemisphere above the aperture of the mass spectrometer. Since the getter is not effective for noble gases, these molecules would be counted if they enter the aperture of the instrument. There are quantities of He stored in pressure spheres behind the aft bulkhead, and the contamination survey conducted with the IECM and the remote manipulator system during STS-4 indicated a significant amount of He and A evolving from this region. If one assumes that the source rate for He identified in Table 4 is confined to the aft bulkhead, the source function would be  $3.1 \times 10^{13}$  molecules/cm<sup>2</sup>/sec. The aft bulkhead subtends approximately 0.025 sr from the entrance aperture at an average angle of ~85°. The flux entering the aperture would be

$$\phi = \frac{3.1 \times 10^{13}}{\pi} 0.025 \cos 85^\circ = 2 \times 10^{10} \text{ cm}^{-2} \text{ sec}^{-1}.$$

This corresponds to a pressure of  $2 \times 10^{-11}$  Torr, which is the measured value. Similarly, if the source of argon observed during the payload bay door closing were confined to the aft bulkhead, Q would be  $7.6 \times 10^{11}$  molecules cm<sup>-2</sup> sec<sup>-1</sup> and the flux entering the instrument aperture would be  $5.3 \times 10^8$  molecules cm<sup>-2</sup> sec<sup>-1</sup>. This would correspond to an equivalent pressure of  $1.6 \times 10^{-12}$  Torr which is close to the observed value of  $1.1 \times 10^{-12}$  Torr. The source of this argon is not clear since argon is not used anywhere in the shuttle system. It was first thought that argon might be a contaminant in the He used for pressurization, but a check with the vendor revealed that the gaseous He supplied for use on shuttle was obtained from liquid He boiloff and contained less than 1 p/m argon. It is interesting to note that the ratio of He to argon observed in the wake is approximately the same as observed in the ram direction. It may be that the source of these molecules in the wake is off-gassing from the aft bulkhead after exposure to the ram flux.

#### CONCLUSIONS

The IECM mass spectrometer flown on STS-3 indicated an upper limit of  $4 \times 10^{-10}$  Torr in the wake of STS-3. This upper limit is set by the instrument background resulting from the zirconia getters in the collimator. Analysis indicates a worst-case estimate of  $2 \times 10^{-10}$  Torr background from atomic oxygen backscattered from the N<sub>2</sub>-induced atmosphere. Direct measurements are needed to determine the actual atomic oxygen background since the scattering efficiencies are not well known at the collision energies involved. Unexpected helium and argon levels at  $2 \times 10^{-11}$  Torr and  $1 \times 10^{-12}$  Torr, respectively, were observed in the wake presumably from the portion of the aft bulkhead in the field-of-view of the instrument. By moving an experiment above the payload bay using the remote manipulator arm it should be possible to achieve vacuum levels in the  $10^{-11}$  Torr range using the existing space shuttle. Ultimate vacuums in the  $10^{-13}$ - $10^{-14}$  Torr range will require remote wake shields or free-flying satellites.

# APPENDIX A

For an observer moving with velocity  $\vec{v}_0$  relative to a system in which molecules have a Maxwell-Boltzmann distribution  $f(\vec{v})$  such that  $\langle \vec{v} \rangle = 0$ , the distribution function may be written

$$d^3 f(\vec{v}') = n \left( \frac{m}{2\pi kT} \right)^{3/2} e^{-\frac{m}{2kT} (\vec{v}' + \vec{v}_0)^2} d^3 \vec{v}' \quad (A1)$$

where  $\vec{v}' = \vec{v} - \vec{v}_0$ .

In the moving system the number of molecules whose motion is within the element of solid angle in the direction  $\theta$  relative to  $\vec{v}_0$  is found by replacing  $d^3 \vec{v}'$  with  $v'^2 d\Omega dv'$ , or

$$\frac{df(\vec{v}')}{d\Omega} \Big|_{\theta} = n \left( \frac{m}{2\pi kT} \right)^{3/2} e^{-\frac{m}{2kT} (\vec{v}' + \vec{v}_0)^2} v'^2 dv' \quad (A2)$$

The vector quantity  $(\vec{v}' + \vec{v}_0)^2$  may be written

$$(\vec{v}' + \vec{v}_0)^2 = v'^2 - 2v' v_0 \cos \theta + v_0^2 \quad (A3)$$

The directional flux of molecules is given by

$$\frac{d\Phi}{d\Omega}(\theta, v') dv' = v' \frac{df(\vec{v}')}{d\Omega} \Big|_{\theta}$$

or

$$\frac{d\Phi}{d\Omega} \Big|_{\theta} = \frac{nv_0}{\pi^{3/2}} \beta^{3/2} \int_0^{\infty} x^3 e^{-\beta(x^2 - 2x \cos \theta + 1)} dx$$

where  $x = v'/v_0$  and  $\beta = mv_0^2/2kT$ . The total flux on the ram face of a plate moving through a Maxwell-Boltzmann gas is given by



$$\begin{aligned}
\phi_{\text{ram}} &= 2\pi \int_0^{\pi/2} \sin \theta \cos \theta \left( \frac{d\phi}{d\Omega} \right)_{\theta} d\theta \\
&= \frac{2nv_o}{\pi^{1/2}} \beta^{3/2} \int_0^{\infty} dx x^3 e^{-\beta(x^2 + 1)} \int_0^{\pi/2} d\theta \sin \theta \cos \theta e^{2\beta x \cos \theta} \\
\phi_{\text{ram}} &= \frac{nv_o}{2} \left[ \frac{e^{-\beta}}{(\pi\beta)^{1/2}} + 1 + \text{erf}(\beta^{1/2}) \right]
\end{aligned}$$

The overtaking flux on the wake side is given by

$$\begin{aligned}
\phi_{\text{wake}} &= -2\pi \int_{\pi/2}^{\pi} \sin \theta \cos \theta \left( \frac{d\phi}{d\Omega} \right)_{\theta} d\theta \\
&= \frac{-2nv_o}{\pi^{1/2}} \beta^{3/2} \int_0^{\infty} dx x^3 e^{-\beta(x^2 + 1)} \int_{\pi/2}^{\pi} d\theta \sin \theta \cos \theta e^{2\beta x \cos \theta} \\
&= \frac{nv_o}{2} \left[ \frac{e^{-\beta}}{(\pi\beta)^{1/2}} - \text{erfc}(\beta^{1/2}) \right]
\end{aligned}$$

As  $v_o \rightarrow 0$ , both of these expressions reduce to

$$\phi = \frac{n}{2} \left( \frac{2kT}{\pi m} \right)^{1/2} = \frac{n}{4} \left( \frac{8kT}{\pi m} \right)^{1/2} = \frac{N\langle v \rangle}{4}$$

where  $\langle v \rangle$  is the mean thermal speed of the gas.

For  $v_o \gg \langle v \rangle$ ,  $\beta \gg 1$  and the asymptotic expansion for  $\text{erf}(\beta^{1/2})$  may be employed to give

$$\phi_{\text{ram}} = \frac{nv_o}{2} \left[ \frac{e^{-\beta}}{(\pi\beta)^{1/2}} + 1 + 1 - \frac{e^{-\beta}}{(\pi\beta)^{1/2}} + \dots \right] \approx nv_o$$

and

$$\phi_{\text{wake}} = \frac{nv_o}{2} \left[ \frac{e^{-\beta}}{(\pi\beta)^{1/2}} - \frac{e^{-\beta}}{(\pi\beta)^{1/2}} \left( 1 - \frac{1}{2\beta} + \dots \right) \right] \approx \frac{nv_o e^{-\beta}}{4\pi^{1/2} \beta^{3/2}}$$

or

$$\phi_{\text{wake}} \approx \frac{n\langle v \rangle}{8} \frac{e^{-\beta}}{\beta} .$$

## APPENDIX B

### Column Density

Consider an observer  $z_0$  above a disc of radius  $R_0$  from which molecules are evolving at a rate  $Q$  per unit area. Assume the surface acts as a perfectly diffuse (Lambertian) radiator so that the directional distribution function is given by

$$\left. \frac{\partial N}{\partial \omega} \right|_{\theta} = \frac{Q \, dA \, \cos \theta}{\pi} \quad (B1)$$

which is the number of molecules per unit time emitted from an element into solid angle  $\partial \omega$  in a direction  $\theta$  from the surface normal. We wish to find the number density along the  $z$  axis of the disc and the integrated column density above  $z_0$ .

The contribution to number density from an element located at some distance  $y$  from the  $z$ -axis at  $z$  is

$$dn_{(y,z)} = \frac{dN}{\Delta V}(y,z) = \left( \left. \frac{\partial N}{\partial \omega} \right|_{y,z} \frac{\Delta \omega}{\Delta V} \right) \langle \tau \rangle$$

where  $\Delta V$  is the volume of the element in question and  $\langle \tau \rangle$  is the average time the molecules remain in the volume. Since  $\Delta V = r^2 \Delta \omega \, dr$ ,  $\langle \tau \rangle = dr \langle v^{-1} \rangle$ ,  $r^2 = y^2 + z^2$ ,  $\cos \theta = z/r$ , and  $dA = 2\pi y \, dy$ ,

$$dn_{(y,z)} = \frac{Q \langle v^{-1} \rangle z \, dA}{\pi (y^2 + z^2)^{3/2}}$$

and

$$\begin{aligned} n_{(z)} &= 2Q \langle v^{-1} \rangle z \int_0^{R_0} \frac{y \, dy}{(y^2 + z^2)^{3/2}} \\ &= 2Q \langle v^{-1} \rangle \left( 1 - \frac{z}{(z^2 + R_0^2)^{1/2}} \right). \end{aligned} \quad (B2)$$

If a Maxwellian distribution is assumed, it is easy to show that

$$\langle v^{-1} \rangle = \frac{4}{\pi \langle v \rangle}$$

where  $\langle v \rangle = \left( \frac{8kT}{\pi m} \right)^{1/2}$  or the average thermal velocity. Hence

$$n(z) = \frac{8Q}{\pi \langle v \rangle} \left[ 1 - \frac{z}{(z^2 + R_o^2)^{1/2}} \right] \quad (B3)$$

The integrated column density is given by

$$N_c = \int_{z_o}^{\infty} n(z) dz = \frac{8Q}{\pi \langle v \rangle} \left[ (z_o^2 + R_o^2)^{1/2} - z_o \right] \quad (B4)$$

A useful relationship between  $N_c$  and  $n(z)$  can be obtained by combining the last two expressions,

$$n(z) = \frac{N_c}{R^*} \left[ 1 - \frac{z}{(z^2 + R_o^2)^{1/2}} \right] \quad (B5)$$

where  $R^* = (z_o^2 + R_o^2)^{1/2} - z_o$ .

#### REFERENCES

1. Wuenschel, H. F.: Manufacturing in Space. New Scientist, Vol. 10, 1970, p. 514.
2. Hueser, J. E. and Brock, F. J.: Theoretical Analysis of the Density within an Orbiting Wake Shield. J. Vac. Sci. Technol., Vol. 13, 1976, p. 702.
3. Oran, W. A. and Naumann, R. J.: Utilization of the Vacuum Developed in the Wake Zone of Space Vehicles in the LDEF Class. J. Vac. Sci. Technol., Vol. 14, 1977, p. 1276.
4. Vaughan, W. W.: Natural Environment Design Criteria for the Space Station Definition and Preliminary Design (First Revision). NASA TM-86460, September 1984.
5. Melfi, L. T. and Outlaw, R. A.: Molecular Shield: An Orbiting Low-Density Materials Laboratory. J. Vac. Sci. Technol., Vol. 13, 1976, p. 648.
6. Miller, E. R. (Editor): STS-2, -3, -4 Induced Environment Contamination Monitor (IECM) Summary Report. NASA TM-82524, February 1983.
7. Carignan, G. R., Block, B. P., Maurer, J. C., Heden, A. E., Reber, C. A., and Spencer, N. W.: The Neutral Mass Spectrometer on Dynamics Explorer B. Space Sci. Instrum., Vol. 5, 1981, p. 429.
8. Wulf, E. and von Zahn, U.: Behavior of Contaminant Gases Emitted by the Space Shuttle and the Manned Maneuvering Unit. Paper presented at the Space Shuttle Experiment and Environmental Workshop, New England College, Henniker, New Hampshire, August 1984.
9. Narcisi, R., Trzcinski, E., Federico, G., Wlodyka, L., and Delory, D.: The Gaseous and Plasma Environment Around the Space Shuttle. Paper presented at the AIAA Shuttle Environment and Operations Meeting, Washington, D.C., October-November 1983.
10. Carignan, G. R. and Dacher, T.: Neutral Composition in the Polar Thermosphere: Observations Made on Dynamics Explorer. Geophys. Res. Lett., Vol. 9, 1982, p. 949.

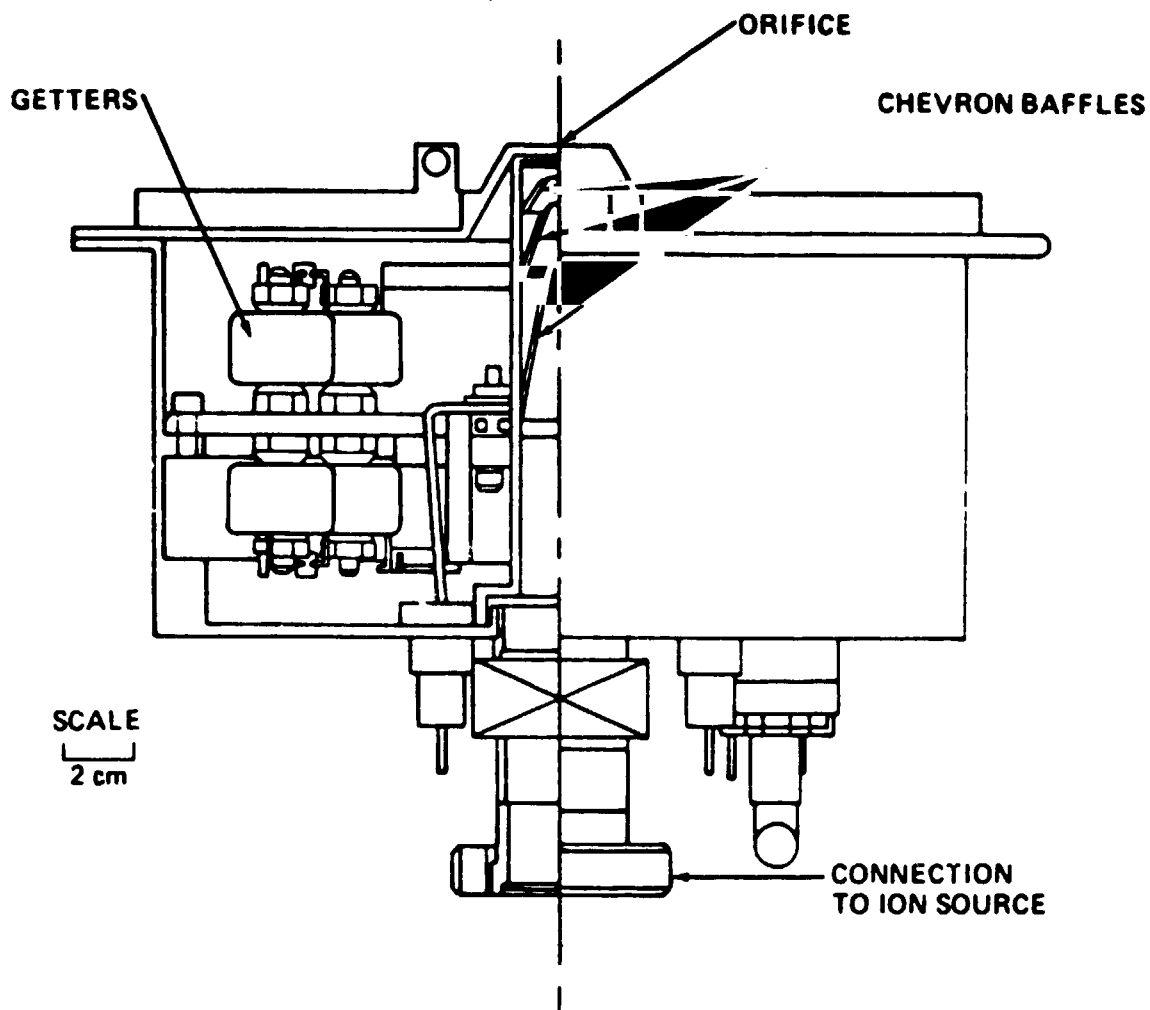


Figure 1. Collimator for the IECM mass spectrometer. The three chevron baffles and zirconia getters remove off-axis molecules and provide a 0.1 sr field-of-view. These getters also provide a low-level background when the instrument is aimed in the "wake" direction. Noble gases are not affected by this collimator.

TABLE 1. AMBIENT ENVIRONMENT OF AN ORBITING VEHICLE AT 250 km

Constituent	Number Den. ( $\text{cm}^{-3}$ )	<sup>1</sup> Ambient Pressure (Torr)	Ram Flux ( $\text{cm}^{-2} \text{sec}^{-1}$ )	Equiv. Ram Pres. (Torr)	Wake Flux ( $\text{cm}^{-2} \text{sec}^{-1}$ )	Equiv. Wake Pres. (Torr)
H	$8.0 \times 10^5$	$8.3 \times 10^{-11}$	$6.2 \times 10^{11}$	$3.0 \times 10^{-10}$	$2.9 \times 10^8$	$1.4 \times 10^{-13}$
He	$6.8 \times 10^6$	$7.0 \times 10^{-10}$	$5.2 \times 10^{12}$	$5.1 \times 10^{-9}$	$5.9 \times 10^3$	$5.7 \times 10^{-18}$
O	$2.0 \times 10^9$	$2.1 \times 10^{-7}$	$1.5 \times 10^{15}$	$2.9 \times 10^{-6}$	$3.2 \times 10^{-12}$	$6.6 \times 10^{-33}$
N <sub>2</sub>	$1.4 \times 10^9$	$1.4 \times 10^{-7}$	$1.1 \times 10^{15}$	$2.9 \times 10^{-6}$	-	-
O <sub>2</sub>	$2.0 \times 10^8$	$2.1 \times 10^{-8}$	$1.5 \times 10^{14}$	$4.2 \times 10^{-7}$	-	-
A	$1.6 \times 10^6$	$1.6 \times 10^{-10}$	$1.2 \times 10^{12}$	$3.7 \times 10^{-9}$	-	-
Total	$3.6 \times 10^9$	$3.7 \times 10^{-7}$	$2.7 \times 10^{15}$	$6.2 \times 10^{-6}$	$2.9 \times 10^8$	$1.4 \times 10^{-13}$

<sup>1</sup>Upper limit values.

<sup>2</sup>Assuming ideal gas at 1000 K and no relative motion.

<sup>3</sup>The pressure of an ideal gas at 300 K corresponding to the estimated flux value.

TABLE 2. SUMMARY OF MEASURED ENVIRONMENT OF VARIOUS MISSIONS

	Measured He Ram Flux ( $\text{cm}^{-2} \text{ sec}^{-1}$ )	Calc. <sup>1</sup> He Ram Flux ( $\text{cm}^{-2} \text{ sec}^{-1}$ )	Observed <sup>2</sup> Ram/Wake Ratio (He) (-)	Eq. Wake Pressure (He) (Torr)	Meas. H <sub>2</sub> O <sup>3</sup> Backscatter Near Ram ( $\text{cm}^{-2} \text{ sec}^{-1} \text{ sr}^{-1}$ )	Est. H <sub>2</sub> O Column Den. ( $\text{cm}^{-2}$ )
STS-2	$3.3 \times 10^{12}$	$5.2 \times 10^{12}$	7.5	$4.4 \times 10^{-10}$	$1.8 \times 10^{13}$	$7.2 \times 10^{12}$
STS-3	$2.2 \times 10^{12}$	$5.2 \times 10^{12}$	100	$2.2 \times 10^{-11}$	$2.7 \times 10^{11}$	$1.1 \times 10^{11}$
STS-4	$2.7 \times 10^{12}$	$3.9 \times 10^{12}$	5.7	$3.3 \times 10^{-10}$	$6.7 \times 10^{12}$	$2.7 \times 10^{12}$
SL 1	$7.8 \times 10^{12}$	$5.2 \times 10^{12}$	7	$1.1 \times 10^{-9}$	-	-
Dynamics Exp.	-	-	>1000	$<2.2 \times 10^{-13}$	-	-

<sup>1</sup>Using upper limit values for atmospheric density.

<sup>2</sup>Only STS-3 and Dynamics Explorer flew with an orientation that pointed the instrument near the wake direction.

<sup>3</sup>The aft bulkhead and other instruments were within the acceptance angle of the instrument on SL 1 which contributed to the measured H<sub>2</sub>O flux. This prevented an accurate assessment of the column density. H<sub>2</sub>O was not measured by Dynamics Explorer.



TABLE 3. WAKE ENVIRONMENT OBSERVED ON STS-3

Mass No.	Species	Observed Flux <sup>1</sup>	Equivalent Partial Pressure (Torr) <sup>2</sup>
4	He	$2.2 \times 10^{10} \text{ cm}^{-2} \text{ sec}^{-1}$	$2.2 \times 10^{-11}$
18	H <sub>2</sub> O	$<5.6 \times 10^9 \text{ cm}^{-2} \text{ sec}^{-1} \text{ sr}^{-1}$	$<3.7 \times 10^{-11}$
28	CO + N <sub>2</sub>	$<4.1 \times 10^{10} \text{ cm}^{-2} \text{ sec}^{-1} \text{ sr}^{-1}$	$<3.4 \times 10^{-10}$
32	O <sub>2</sub>	$<3.8 \times 10^7 \text{ cm}^{-2} \text{ sec}^{-1} \text{ sr}^{-1}$	$<3.4 \times 10^{-13}$
40	A	$3.5 \times 10^8 \text{ cm}^{-2} \text{ sec}^{-1}$	$1.1 \times 10^{-12}$

<sup>1</sup>Except for He and A these data represent instrument background and should be regarded as an upper bound. The collimator is not effective for noble gases and for these cases the instrument is calibrated in terms of pressure.

<sup>2</sup>Pressure of an ideal gas in thermal equilibrium with a closed chamber at 300 K that corresponds to the stated directional flux values.

TABLE 4. MEASUREMENTS IN STS-3 PAYLOAD BAY WITH DOORS CLOSED

Species	Measured Pressure (Torr)	Ave. Velocity (m/sec)	Pumping Rate ( $\text{sec}^{-1}$ )	Distributed Source Function ( $\text{cm}^{-2} \text{ sec}^{-1}$ )	Est. Column Density ( $\text{cm}^{-2}$ )
He	$1.5 \times 10^{-7}$	1263	$1.1 \times 10^{18}$	$1.3 \times 10^{12}$	$1.1 \times 10^{10}$
CH <sub>4</sub>	$2.9 \times 10^{-7}$	631	$1.1 \times 10^{18}$	$1.3 \times 10^{12}$	$2.3 \times 10^{10}$
H <sub>2</sub> O	$2.7 \times 10^{-7}$	596	$9.8 \times 10^{17}$	$1.1 \times 10^{12}$	$2.0 \times 10^{10}$
N <sub>2</sub>	$6.0 \times 10^{-6}$	478	$1.7 \times 10^{19}$	$2.0 \times 10^{13}$	$4.6 \times 10^{11}$
O <sub>2</sub>	$3.4 \times 10^{-8}$	447	$9.3 \times 10^{16}$	$1.1 \times 10^{11}$	$2.7 \times 10^9$
A	$1.0 \times 10^{-8}$	400	$2.7 \times 10^{16}$	$3.1 \times 10^{10}$	$8.5 \times 10^8$
CO <sub>2</sub>	$6.2 \times 10^{-9}$	381	$1.4 \times 10^{16}$	$1.6 \times 10^{10}$	$4.6 \times 10^8$

TABLE 5. RELATIVE SCATTERING EFFICIENCIES FOR COLLISIONS OF INTEREST

$M_O$ $M_A$	4	16	18	28	32	40	44	67
1	0.650	0.908	0.917	0.947	0.953	0.962	0.966	0.979
4	-	0.650	0.686	0.793	0.818	0.854	0.867	0.912
16	-	-	0.034	0.280	0.354	0.465	0.508	0.665
28	-	-	-	-	0.041	0.162	0.218	0.445
32	-	-	-	-	-	0.087	0.140	0.378
40	-	-	-	-	-	-	0.025	0.255

TABLE 6. WAKE ENVIRONMENT FROM AMBIENT MOLECULES BACKSCATTERED BY COLLISIONS  
WITH THERMAL MOLECULES IN THE INDUCED ENVIRONMENT

Species	Total Flux ( $\text{cm}^{-2} \text{ sec}^{-1}$ )	Directional Flux at $\theta = \pi$ ( $\text{cm}^{-2} \text{ sec}^{-1} \text{ sr}^{-1}$ )	Equivalent Pressure (Torr)
H	$2.0 \times 10^8$	$9.8 \times 10^7$	$9.8 \times 10^{-14}$
He	$1.3 \times 10^9$	$7.9 \times 10^8$	$1.3 \times 10^{-12}$
O	$9.4 \times 10^{10}$	$1.3 \times 10^{11}$	$1.8 \times 10^{-10}$
N <sub>2</sub>	$1.7 \times 10^8$	$2.9 \times 10^8$	$4.3 \times 10^{-13}$
O <sub>2</sub>	$9.6 \times 10^6$	$1.8 \times 10^7$	$2.6 \times 10^{-14}$
A	$6.5 \times 10^3$	$2.2 \times 10^4$	$2.1 \times 10^{-17}$

TABLE 7. BACKSCATTER FUNCTION  $F(\zeta_o, M)$  FOR  $\zeta_o = 0$  AND  $\zeta_o = 0.2$  (IN PARENTHESES)

$M_1$	$M_2$	4	16	18	28	32	40	44	67
4		0.0081 (0.0012)	0.0902 (0.0383)	0.1019 (0.0453)	0.1501 (0.0760)	0.1651 (0.0860)	0.1896 (0.1024)	0.1998 (0.1093)	0.2414 (0.1371)
16		- (-)	0.0081 (0.0012)	0.0110 (0.0020)	0.0289 (0.0080)	0.0363 (0.0101)	0.0507 (0.0173)	0.0577 (0.0207)	0.0947 (0.0409)
18		(-)	0.0059 (0.0007)	0.0081 (0.0012)	0.0232 (0.0058)	0.0297 (0.0082)	0.0427 (0.0136)	0.0491 (0.0166)	0.0833 (0.0343)
28		- (-)	(0.0008) (-)	0.0017 (0.00005)	0.0081 (0.0012)	0.0114 (0.0022)	0.0194 (0.0046)	0.0236 (0.0060)	0.0476 (0.0158)
32		-	(0.0003)	0.0007	0.0056 (0.0007)	0.0081 0.0012	0.0143 (0.0030)	0.0178 (0.0041)	0.0390 (0.0120)
40		-	-	0.00007 (-)	0.0025 (0.00012)	0.0042 (0.0004)	0.0081 (0.0012)	0.0104 (0.0019)	0.0267 (0.0072)
44		-	-	0.00001 (-)	0.0016 (0.00007)	0.0029 (0.0002)	0.0063 (0.0008)	0.0081 (0.0012)	0.0222 (0.0056)
67		-	-	-	0.000018 (-)	0.00016 (-)	0.0011 (0.00001)	0.0018 (0.00006)	0.0081 (0.0012)

TABLE 8. COMPARISON OF ESTIMATED AND MEASURED WAKE ENVIRONMENT


Species	Estimated Flux (molecules/cm <sup>2</sup> sec)			Equiv. Pressure (Torr)	
	Ambient	Ambient Backscattered	Self-Scattered (Sill Line)	Estimated	Measured
H (1)	$2.1 \times 10^8$	$2.9 \times 10^8$	--	$2.0 \times 10^{-13}$	--
He (4)	$3.6 \times 10^3$	$1.3 \times 10^9$	$4.0 \times 10^7$	$1.3 \times 10^{-12}$	$2.2 \times 10^{-11}$
O (16)	$7.5 \times 10^{-15}$	$9.4 \times 10^{10}$	--	$1.8 \times 10^{-10}$	--
CH <sub>4</sub> (16)	--	--	$3.3 \times 10^7$	$6.5 \times 10^{-14}$	--
H <sub>2</sub> O (18)	--	--	$8.6 \times 10^7$	$1.8 \times 10^{-13}$	$<3.7 \times 10^{-11}$
N <sub>2</sub> + CO (28)	--	$1.7 \times 10^8$	$3.2 \times 10^7$	$5.2 \times 10^{-13}$	$<3.4 \times 10^{-10}$
O <sub>2</sub> (32)	--	$9.6 \times 10^6$	$1.1 \times 10^5$	$3.1 \times 10^{-16}$	$<3.4 \times 10^{-13}$
A (40)	--	$6.5 \times 10^3$	$1.4 \times 10^4$	$6.2 \times 10^{-17}$	$1.1 \times 10^{-12}$
CO <sub>2</sub>	--	--	$3.6 \times 10^3$	$1.8 \times 10^{-18}$	--

APPROVAL

SPACE SHUTTLE MOLECULAR SCATTERING AND WAKE VACUUM MEASUREMENTS

By R. J. Naumann, G. R. Carignan, and E. R. Miller

The information in this report has been reviewed for technical content. Review of any information concerning Department of Defense or nuclear energy activities or programs has been made by the MSFC Security Classification Officer. This report, in its entirety, has been determined to be unclassified.

  
A. J. DESSLER  
Director, Space Science Laboratory